

Modulated charged defects and conduction behaviour in doped BiFeO₃ thin films

This article has been downloaded from IOPscience. Please scroll down to see the full text article.

2009 J. Phys. D: Appl. Phys. 42 162001

(<http://iopscience.iop.org/0022-3727/42/16/162001>)

View [the table of contents for this issue](#), or go to the [journal homepage](#) for more

Download details:

IP Address: 38.107.179.214

The article was downloaded on 22/02/2012 at 01:01

Please note that [terms and conditions apply](#).

FAST TRACK COMMUNICATION

Modulated charged defects and conduction behaviour in doped BiFeO_3 thin films

Y Wang and J Wang¹

Faculty of Engineering, Department of Materials Science and Engineering, National University of Singapore, Singapore 117576

E-mail: msewy@nus.edu.sg, wangyangnju@gmail.com and msewangj@nus.edu.sg

Received 21 May 2009, in final form 30 June 2009

Published 23 July 2009

Online at stacks.iop.org/JPhysD/42/162001**Abstract**

The charged defective structure in $\text{Bi}_{1-x}\text{La}_x\text{FeO}_3$ (BLF) and La-10% and Mg-2% co-doped BiFeO_3 (BLFM) thin films as well as their relations to leakage and dielectric relaxation behaviour are investigated. Through temperature-dependent conductivity and x-ray photoelectron spectroscopy analyses, it is demonstrated that La doping suppresses but Mg doping increases the concentration of both oxygen vacancies (OVs) and Fe^{2+} ions. Correspondingly, the leakage mechanism evolves from grain boundary and space charge limited conduction of BLF ($x = 0.2$ and 0.1) to Poole–Frenkel emission of BLFM and BiFeO_3 . Although the dielectric relaxation originates from the migration of OVs, the formation of defect complexes between the acceptors and OVs is responsible for the increased activation energy of the BLFM film.

(Some figures in this article are in colour only in the electronic version)

Multiferroics, which exhibit simultaneous (anti)ferroelectric and (anti)ferromagnetic orders, have attracted considerable attention in recent years due to the fascinating physics underlying the coupling between ferroelectric polarization and magnetism and the new generation of multiple controlled devices that are promised [1]. Among the multiferroic materials studied, BiFeO_3 (BFO) has attracted extraordinary interest, owing to its high ferroelectric and antiferromagnetic transition temperatures [2, 3]. Indeed, both a large polarization of $60 \mu\text{C cm}^{-2}$ and an electric field control of antiferromagnetic domains have been successfully observed in epitaxial BFO thin films [4, 5]. However, the severe leakage problem of BFO greatly impedes its practical application. Accordingly, several researchers have been focusing their efforts on this problem, which is important and yet difficult to solve. It is basically accepted that leakage current of BFO results mainly from the occurrence of charged defects (V_O^{2+} and Fe^{2+}), which could be efficiently diminished with

chemical doping [6–8]. Meanwhile, several models have been presented to describe the leakage behaviour, including the interface-limited Schottky emission [8], bulk-limited Poole–Frenkel (PF) emission [9] and space charge limited conduction (SCLC) [6]. Interestingly, one may enquire how these charged defects influence leakage behaviour, respectively, and which mechanism is dominant under a certain condition. However, little progress has been made with the answers to these questions. Moreover, it is well known that charged defects may move and pin the domain walls under the drive of an electric field and thus affect the electrical performances of ferroelectric films [10]. Therefore, it is necessary to further identify the charged defective structure of BFO-based films and their migration kinetics. In this work we have modulated the charged defects of BFO films by replacing Bi and Fe with La and Mg, in an attempt to establish their correlations with conduction mechanisms. The dielectric relaxation and migration kinetics of charged defects are also investigated.

¹ Author to whom any correspondence should be addressed.

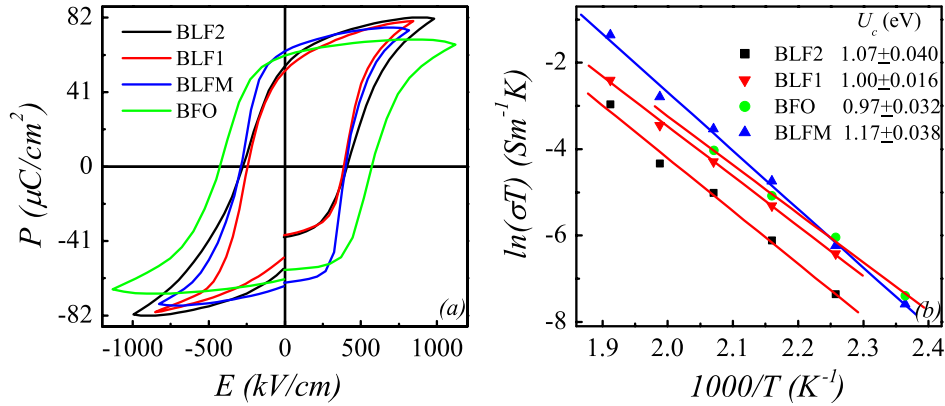


Figure 1. (a) P - E hysteresis loops and (b) temperature-dependent conductivity σ_{dc} for thin film samples. (Colour online.)

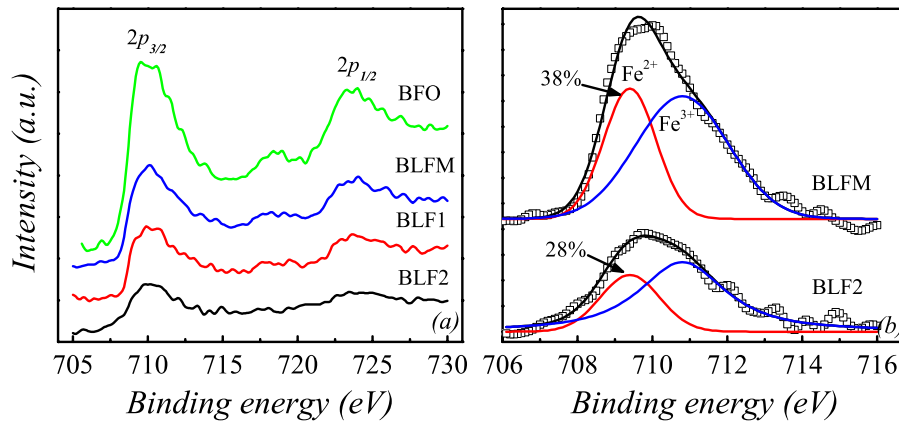


Figure 2. (a) Fe 2p XPS spectra and (b) the peak partition results of Fe $2p_{3/2}$ core level for BLFM and BLF2 films. (Colour online.)

$\text{Bi}_{1-x}\text{La}_x\text{FeO}_3$ ($x = 0, 0.1$ and 0.2 , denoted as BFO, BLF1 and BLF2) and La-10% and Mg-2% co-doped BiFeO_3 (BLFM) thin films were deposited by rf magnetron sputtering on platinumized Si wafers at 650°C with SrRuO_3 as the buffer layer. The detailed procedure of preparation has been described elsewhere [11]. These films were measured to be 220, 350, 230 and 330 nm in thickness for $\text{Bi}_{1-x}\text{La}_x\text{FeO}_3$ ($x = 0.0, 0.1$ and 0.2) and BLFM, respectively, by using scanning electron microscopy (SEM, Philips XL 30). All the films were verified by x-ray diffraction (XRD) to exhibit a polycrystalline structure of the single perovskite phase [11]. The combination states of Fe 2p electron were examined by x-ray photoelectron spectroscopy (XPS). Prior to electrical measurements, Au dots of $200\ \mu\text{m}$ diameter were sputtered on the films as top electrodes. A Solartron impedance analyzer was employed to measure complex impedance spectroscopy (CIS), and the leakage current was studied by using a Keithley 6430 I - V system. The polarization-electric field (P - E) hysteresis loops were characterized with a Radiant precise workstation.

Figure 1(a) demonstrates the well-saturated P - E loops for four thin films, respectively, giving the remanent polarization $2P_r$ of 110 - $120\ \mu\text{C}\ \text{cm}^{-2}$. These large values agree well with those reported [4, 9], and confirms the desired ferroelectricity of these films. The conductivity σ_{dc} arises from the ordered migration of charged species, and thus its dependence on temperature T can reveal the type and density of

charge carriers manipulating the conductivity process. CIS is effective in revealing the electrical response in polycrystalline materials [12], which can give the dc resistance values through the low frequency intercepts on real axis. Therefore, CIS was measured at different T for the thin films and the calculated σ_{dc} versus T are presented in figure 1(b), which can be expressed as $\sigma_{dc} = nq\mu \propto T^{-1} \exp(-U_c/k_B T)$, where n is the density of carriers, q is the carrier charge, μ is the mobility, U_c is the activation energy of carrier migration and k_B is the Boltzmann constant. The solid lines are the fitting results. From the slopes the values of U_c are evaluated to be $\sim 1.0\ \text{eV}$. Previous works point out the activation energy related to oxygen vacancies (OVs) is $0.9\ \text{eV}$ for BFO [13] and 0.98 - $1.13\ \text{eV}$ for SrTiO_3 [14]. Hence, the close agreement of U_c obtained in this work with those reported validates the conductivity in BFO-based films arises from OVs, and the larger σ_{dc} of the BLFM and BFO films in contrast to that of BLF2 and BLF1 implies the higher density of OVs. According to the defect equilibrium: $\text{O}_o \leftrightarrow 0.5\text{O}_2 + \text{V}_o^{\cdot\cdot} + 2e'$ and $\text{Fe}^{3+} + e' \leftrightarrow \text{Fe}^{2+}$, a change in OVs will affect the oxidation state of Fe ions to meet electrical neutrality, and they both contribute to the leakage current. As XPS can be used to identify the chemical states of Fe, figure 2(a) plots the Fe 2p XPS spectra for four films. Clearly, due to the spin-orbit coupling, the Fe 2p core level is split into $2p_{1/2}$ and $2p_{3/2}$ components. Because the binding energy of Fe $2p_{3/2}$ is expected to be $709.4\ \text{eV}$ for Fe^{2+} and $710.8\ \text{eV}$ for Fe^{3+} , the asymmetric broadband centred at $\sim 710\ \text{eV}$ manifests

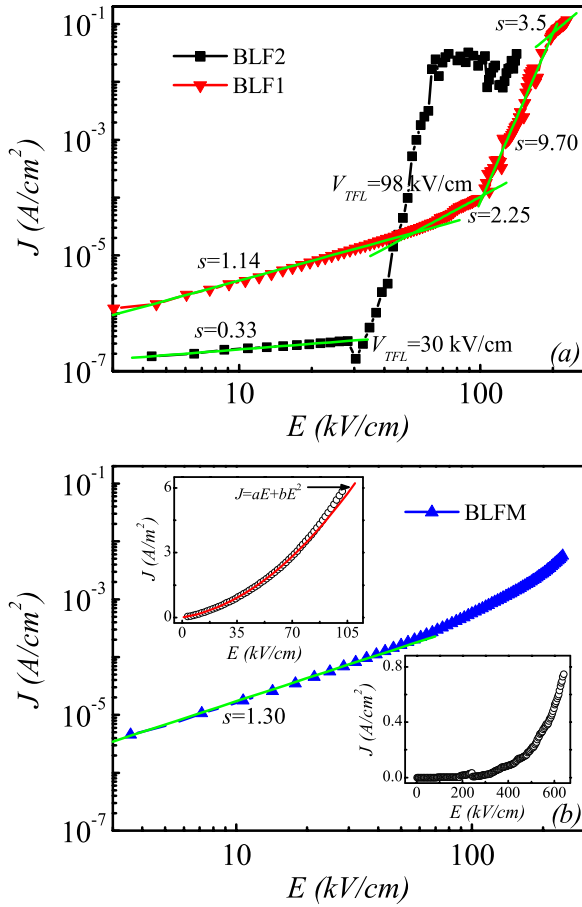


Figure 3. The log J –log E curves and the upper and lower insets in (b) show a Langmuir–Child fitting of J – E curve and the exponentially increased J at high E for BLFM film, respectively. (Colour online.)

the coexistence of Fe^{2+} and Fe^{3+} , and the peak partition using Gaussian–Lorentzian profile gives Fe^{2+} percentage in the bulk to be 28%, 24%, 38% and 37% for BLF2, BLF1, BLFM and BFO, respectively, as shown in figure 2(b). On the basis of the T -dependent σ_{dc} and XPS analysis, one can conclude that La doping suppresses the generation of OV and subsequently the conversion of Fe^{3+} to Fe^{2+} , whereas Mg doping facilitates the formation of both OV and Fe^{2+} . The change in the concentrations of OV and Fe^{2+} can also be further comprehended as follows. Given that the OV is positively charged, it will be an electron attraction site, and the association of any free electron will reduce Fe^{3+} in the vicinity of OV into Fe^{2+} . Since the Mg–O bond ($\sim 363 \text{ kJ mol}^{-1}$) possesses a relatively weaker chemical bonding than that of the Fe–O bond ($\sim 390 \text{ kJ mol}^{-1}$), Mg substitution for Fe makes the oxygen in the octahedron less stable and facilitates the formation of OV. The increased concentration of OV will apparently enhance the probability for electrons to be captured by OV, leading to the increased Fe^{2+} concentration in BLFM film.

Leakage current density J as a function of electric field E was measured and plotted as logarithmic curves in figures 3(a) and (b). Several previous researchers have proposed SCLC in their works [6]. Distinctly, the log J –log E curve of the BLF1

film can be well fitted by four linear segments with different slopes, known as a typical SCLC with deep trap levels [15]. At low E , the thermally activated free electrons predominate, leading to a linear Ohmic relationship. With the increase in E , when the density of injected free electrons exceeds that of thermally excited free electrons, SCLC will take over the leakage behaviour and a modified Child’s law is observed [15],

$$j_{\text{SCL}} = 9\varepsilon\varepsilon_0\mu\theta V^2/8d^3, \quad (1)$$

where ε is the dielectric constant, ε_0 is the permittivity of free space, V is the applied voltage, d is the film thickness and θ is the ratio of free carrier density to the total carrier density. Hence, the derived slope of 2.25 signifies a square-law dependence. In this region, the injected electrons are largely captured by the traps locating in the band gap, which explains the origin of parameter θ . Afterwards, when the voltage reaches a particular value where all the traps get filled, an abrupt increase in J occurs followed by a saturation-like region with a slope of 3.5, which is larger than slope 2 for a full Child’s relationship. This crossover voltage is the trap-filled-limit (V_{TFL}), related to the trap density N_t by $V_{\text{TFL}} = 2eN_t d^2/3\varepsilon\varepsilon_0$. Comparing log J –log E curves of BLF1 and BLF2 films, one can observe that V_{TFL} declines from 98 kV cm^{-1} of BLF1 to 30 kV cm^{-1} of BLF2, elucidating a lower density of traps in BLF2, namely less OV, since the electron traps in perovskite films are largely created by OV [16]. Consistently, when $E < 30 \text{ kV cm}^{-1}$, the observed slope of less than unity for BLF2 indicates a grain boundary limited behaviour, which has been reported in Nb-doped BFO film and ascribed to the low concentration of OV [7]. For BLFM film, the linearity is observed at the low E , and the upper inset in figure 3(b) demonstrates that the J – E curve up to 70 kV cm^{-1} could be well depicted by the modified Langmuir–Child law [17], confirming SCLC indeed operates here. In addition, as compared with BLF2, BLF1 and BLFM films demonstrate the larger J at low E , because more OV gives birth to more traps from which more electrons get excited.

The J – E curve of the BLFM film reveals an exponential increase at the high E , just as shown in the lower inset of figure 3(b), indicating the operation of another predominant mechanism, where the Schottky emission and PF emission have to be considered and given by [9]

$$j_s = AT^2 \exp[-(\Phi - \beta E^{1/2})/k_B T], \quad (2)$$

$$j_{\text{PF}} = BE \exp[-(E_1 - \beta E^{1/2})/k_B T], \quad (3)$$

where A and B are both constants, Φ is the height of Schottky barrier, E_1 is the trap ionization energy, $\beta = (q^3/\alpha\pi\varepsilon_0 K)^{1/2}$, q is the electron charge, K is the optical dielectric permittivity and $\alpha = 4$ for Schottky and 1 for PF emission, respectively. Recalling that Schottky and PF emission are characterized by the linear fits of $\ln J$ – $E^{0.5}$ and $\ln(J/E)$ – $E^{0.5}$, respectively, these two relationships are illustrated in figure 4(a), both complying with a linear dependence. Thus, to determine which one mechanism governs the high- E leakage current, the derived K value should be considered, which will coincide with the intrinsic material property. From the slopes of

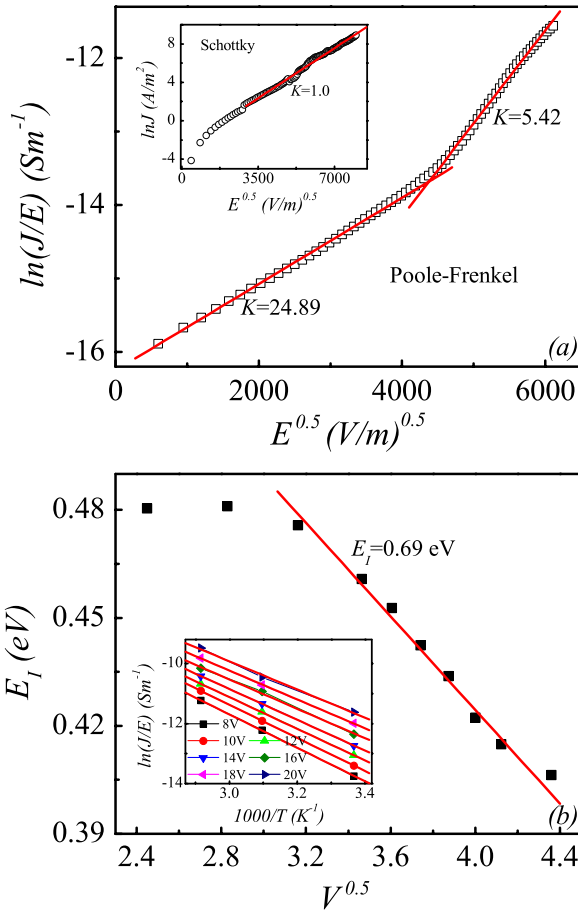


Figure 4. (a) The plots of $\ln J-E^{0.5}$ and $\ln(J/E)-E^{0.5}$ for Schottky and PF emission mechanisms. (b) The voltage-dependent trap ionization energy calculated from $\ln(J/E)$ versus T . (Colour online.)

the linear fittings, the value of K is calculated to be 24.89 below 140 kV cm^{-1} and 5.42 above 200 kV cm^{-1} for the PF mechanism, while the Schottky plot yields a value of 1.0 at high E . Recently, the K value of BFO has been estimated to be 6.25 from the refractive index of $n = 2.5$ [18]. The obtained value of 5.42 is in reasonable agreement, suggesting that the conduction of the BLFM film above 200 kV cm^{-1} is controlled by PF emission, which involves the thermally and electrically assisted continuous hopping of charges between defect trap sites, such as $\text{Fe}^{2+}/\text{Fe}^{3+}$ ions in BFO. Accordingly, to further confirm the validity of PF emission, we have measured $J-E$ curves at the different T and plotted the voltage-dependent trap ionization energy in figure 4(b), from which the zero-field E_1 is extrapolated to be 0.69 eV. Indeed, Pabst *et al* also reported the PF emission in BFO film and derived E_1 of 0.65–0.8 eV [9]. Both BLFM and BFO films exhibit a high concentration of Fe^{2+} ions, and the above described results appear reasonable. Accordingly, it can be concluded that the leakage behaviour of BFO-based films is markedly affected by the charged defects, which changes from SCLC of BLF to PF emission of BLFM and BFO under the modulation of chemical doping.

Moreover, the charged defects inevitably interact with their neighbourhood, where the migration involves the relaxation process besides the conductance. Thereby, an

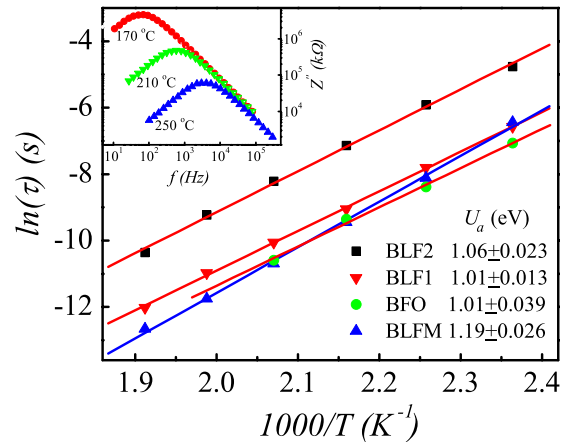


Figure 5. The relaxation time τ versus $1/T$ and the inset shows the variation of the imaginary part Z'' of impedance with frequency at different T for BLF2 film. (Colour online.)

investigation into the dielectric relaxation will provide one with further insight into the charged defects structure and their migration kinetics. The imaginary part Z'' of the impedance of the BLF2 film presented in the inset of figure 5 typifies a thermally excited relaxation, demonstrating a notable low frequency f dispersion and T -dependent peak frequency f_{max} . The relaxation time τ versus $1/T$ is plotted in figure 5, where the excellent linear fittings suggest an Arrhenius correlation: $\tau = 1/2\pi f_{\text{max}} = \tau_0 \exp(-U_a/k_B T)$, where τ_0 is the pre-exponential factor and U_a is the activation energy required for relaxation. The values of U_a for film samples are evaluated to be ~ 1.0 eV, showing that the essential elements responsible for the relaxation process belong to OVs. Nevertheless, further inspecting figures 1(b) and 5, one can note that as compared with BLF2, BLF1 and BFO possess a smaller activation energy and a shorter τ . According to the point defect relaxation theory [19], there exists an interaction among OVs, which have been considered to favour their migration. Thus, a stronger correlation in association with a higher density of OVs would facilitate the movement lowering U_c and τ . However, contradictorily, the BLFM film with the highest density of OVs demonstrates the largest U_a and U_c , implying the existence of other factors contributing to the relaxation process. For conventional perovskite titanate, it has been shown that OVs can couple with Ti^{3+} ions to form defect complexes [14]. Thus, a level of extra energy is required to overwhelm the electrostatic attraction force between OVs and the acceptors before OVs become mobile. Since BLFM film comprises Mg^{2+} ions, which serve as the acceptors, it can be concluded that they are combined with OVs to build up defect complexes, which elevate the activation energy of OVs in the BLFM film and increase τ at low T .

In summary, we have studied the charged defects structure in La/Mg-doped $\text{Bi}_{1-x}\text{La}_x\text{FeO}_3$ thin films, in an attempt to establish their correlations with the leakage mechanism and dielectric relaxation behaviour. It is illustrated that La doping suppresses but Mg doping increases the concentration of both OVs and Fe^{2+} ions. Consequently, the leakage mechanism evolves from the grain boundary conduction and SCLC of BLF to PF emission of BLFM and BFO. The formation of defect

complexes between the acceptors and OV's can account for the high activation energy of BLFM film, while the dielectric relaxation originates from the migration of OV's.

Acknowledgments

Dr Wang Yang is supported by the Singapore Millennium Foundation. The authors acknowledge the support of the National University of Singapore.

References

- [1] Cheong S W and Mostovoy M 2007 *Nature Mater.* **6** 13
- [2] Binek C and Doudin B 2005 *J. Phys. Condens. Matter* **17** L39
- [3] Venevtsev Yu N, Zhadanov G and Solov'ev S 1960 *Sov. Phys. Crystallogr.* **4** 538
- [4] Smolenskii G, Yudin V, Sher E and Stolypin Yu E 1963 *Sov. Phys.—JETP* **16** 622
- [5] Wang J *et al* 2003 *Science* **299** 1719
- [6] Zhao T *et al* 2006 *Nature Mater.* **5** 823
- [7] Qi X D, Dho J H, Tomov R, Blamire M G and MacManus-Driscoll J L 2005 *Appl. Phys. Lett.* **86** 062903
- [8] Chung C F, Lin J P and Wu J M 2006 *Appl. Phys. Lett.* **88** 242909
- [9] Quan Z, Liu W, Hu H, Xu S, Sebo B, Fang G J, Li M Y and Zhao X Z 2008 *J. Appl. Phys.* **104** 084106
- [10] Pabst G W, Martin L W, Chu Y H and Ramesh R 2007 *Appl. Phys. Lett.* **90** 072902
- [11] Wu D, Yuan G L and Li A D 2007 *Appl. Phys. Lett.* **90** 062902
- [12] Wang Y, Zheng R Y, Sim C H and Wang J 2009 *J. Appl. Phys.* **105** 016106
- [13] Lanfredi S and Rodrigues A C M 1999 *J. Appl. Phys.* **86** 2215
- [14] Yan Z, Wang K F, Qu J F, Wang Y, Song Z T and Feng S L 2007 *Appl. Phys. Lett.* **91** 082906
- [15] Morii K, Kawano H, Fujii I, Matsui T and Nakayama Y 1995 *J. Appl. Phys.* **78** 1914
- [16] Rose A 1955 *Phys. Rev.* **97** 1538
- [17] Lampert M A 1956 *Phys. Rev.* **103** 1648
- [18] Choi D, Lee D, Sim H, Chang M and Hwang H 2006 *Appl. Phys. Lett.* **88** 082904
- [19] Tredgold R H 1966 *Space Charge Conduction in Solids* (Amsterdam: Elsevier)
- [20] Iakovlev S, Solterbeck C-H, Kuhnke M and Es-Souni M 2005 *J. Appl. Phys.* **97** 094901
- [21] Nowick S and Berry B S 1972 *Anelastic Relaxation in Crystalline Solids* (New York: Academic)